

# Optimal BESS Allocation in Large Transmission Networks Using Linearized BESS Models

Malhar Padhee and Anamitra Pal

School of ECEE

Arizona State University, USA

[mpadhee@asu.edu](mailto:mpadhee@asu.edu), [anamitra.pal@asu.edu](mailto:anamitra.pal@asu.edu)

Chetan Mishra

Electric Transmission Op. Engineering

Dominion Energy, USA

[chetan.mishra@dominionenergy.com](mailto:chetan.mishra@dominionenergy.com)

Sachin Soni

Grid Integration

First Solar, USA

[sachin.soni@firstsolar.com](mailto:sachin.soni@firstsolar.com)

**Abstract**—The most commonly used model for battery energy storage systems (BESSs) in optimal BESS allocation problems is a constant-efficiency model. However, the charging and discharging efficiencies of BESSs vary non-linearly as functions of their state-of-charge, temperature, charging/discharging powers, as well as the BESS technology being considered. Therefore, constant-efficiency models may inaccurately represent the non-linear operating characteristics of the BESS. In this paper, we first create technology-specific linearized BESS models derived from the actual non-linear BESS models. We then incorporate the linearized BESS models into a mixed-integer linear programming framework for optimal multi-technology BESS allocation. Studies carried out on a 2,604-bus U.S. transmission network demonstrate the benefits of utilizing the linearized BESS models from the model accuracy, convexity, and computational performance viewpoints.

**Index Terms**—Linearized BESS model, Lithium-ion, Mixed-integer linear program, Optimal BESS allocation, Solar photovoltaic, Vanadium redox flow.

## I. INTRODUCTION

The utilization of renewable energy resources for bulk power generation has seen a rapid growth over the last few decades. With more than 15 GW of solar photovoltaic (PV) to be installed annually till 2024, it is anticipated that the total installed PV capacity will more than double in the next five years [1]. However, the intermittency of renewable energy resources may create imbalances in power supply and demand, detrimentally affecting the bulk power system (BPS)'s reliability and stability. Considering such impacts, energy storage systems (ESSs) are a feasible solution, as they can act as buffers to help mitigate the variability of renewable resources. However, it is essential to optimally allocate ESSs, particularly for BPSs, owing to the relatively high initial capital and maintenance costs for ESSs, e.g., battery ESSs (BESSs) [2]. System-wide benefits, e.g., mitigation of line congestion and deferral of transmission upgrades can also be obtained through optimal BESS allocation.

Refs. [3]-[9] solved the optimal BESS allocation problem for transmission networks in order to minimize generation cost, optimize storage portfolio, or transmission expansion investments. Refs. [9]-[12] have dealt with optimal BESS allocation in microgrids and distribution networks. However, the linear constant-efficiency BESS models used in [3]-[12] are not realistic since the nature of BESS operation depends on

the technology being considered, whose efficiencies vary non-linearly with the charging and discharging powers, state-of-charge (SOC), and temperature [13]-[16]. Moreover, [13], [14] showed that, when compared with the non-linear BESS models, the linear constant-efficiency models provided inaccurate representations of the BESS's economic benefits in short-term power system operation problems. Therefore, one should model the diverse non-linear operating characteristics of BESSs for an accurate assessment of the techno-economic benefits of such technologies. In the past, non-linear BESS models have been utilized in SOC estimation and control applications [17]-[19]. However, these models focus on the non-linear fast dynamics of BESSs and are unsuitable for techno-economic analyses in short/long-term planning studies.

Ref. [13] quantified the benefits of incorporating technology-specific BESS models (Vanadium redox flow (VRF) and Lithium-ion (LI) BESSs) in power system optimization problems. However, the non-linear BESS operation models utilized in [13] make it very difficult to integrate them in large-scale power system planning problems as they become non-convex (potentially resulting in multiple locally optimal/sub-optimal solutions) and computationally intractable. Refs. [14]-[16] demonstrated the usage of piecewise linearization for building linear operation models of LI BESSs by starting from the original non-linear operation models. However, binary variables introduced by the BESS optimization models would render them unsuitable for large-scale transmission planning problems, such as the one being studied here. Based on the aforementioned research gaps, this paper makes the following salient contributions:

1. Development of a novel linearized scenario-based BESS allocation scheme that incorporates accurate linear programming (LP) models of two different BESSs (VRF and LI) which provide complementary benefits [2].
2. Performance evaluation of the proposed scheme for BESS siting and sizing using a real U.S. transmission network with regards to different BESS modeling approaches.

The rest of the paper is organized as follows. Section II describes the proposed linearized scenario-based problem formulation to allocate multiple BESS technologies. Section III builds LP operation models of the original non-linear VRF and LI BESS models for integration into the proposed BESS planning scheme. Section IV contains optimal BESS allocation results demonstrating the various benefits of using the

proposed LP BESS models over other BESS models. Lastly, Section V presents the concluding comments.

## II. PROPOSED SCENARIO-BASED PROBLEM FORMULATION FOR MULTI-TECHNOLOGY BESS ALLOCATION

Prior to solving large transmission planning problems, it is important to efficiently generate realistic uncertain solar PV power output and load scenarios. To learn the spatio-temporal correlations between system loads from actual load data, [20] proposed the usage of principal component analysis (PCA) and topology-based metrics. New synthetic load data with characteristics comparable to real load could be generated using that model. In [21], [20]'s approach was enhanced for modeling seasonal variations in both wind power output and system load. In this paper, the algorithm developed in Section III-A of [21] is applied to solar PV as well as load scenario generation. Real hourly data of power output from multiple solar farms and system load data for eleven years (2009-2019) was collected from a large power utility operating in the U.S. Southwest. A scenario reduction technique called submodular scenario reduction (SSR) [22] was used to identify representative solar PV power and load scenarios.

The scenarios of solar PV power output and system load generated previously (see [21] for more details) are utilized in formulating the optimal VRF and LI BESS allocation problem. The transmission network is also equipped with capacitor banks which participate in attaining the desired objectives (minimize bus voltage fluctuations, lower operation costs); as such, their operations are also appropriately modeled in the optimization formulation. The problem formulation is given below, where (1) is the objective function.

$$\text{Min: } C_T = C_{OP} + C_{IB} + C_{RB} \quad (1a)$$

$$C_{OP} = \sum_{\psi=1}^{\Xi} p^{\psi} \left[ \sum_{t=1}^T \left\{ \sum_{g=1}^{N_g} CG_{g,t}^{\psi} + c_{em} \sum_{g=1}^{N_g} PG_{g,t}^{\psi} + cp_l \sum_{l=1}^{N_l} Pl_{l,t}^{\psi} + c_{sp} \sum_{g=1}^{N_g} SP_{g,t}^{\psi} + \sum_{j=1}^N (cv_j) BV_{j,t}^{\psi} + c_{cap} \sum_{j=1}^N (Pd_{j,t}^{\psi} \Delta t + Pc_{j,t}^{\psi} \Delta t + ES_{j,t}^{\psi} \cdot \eta_{LL}) \right\} \right] \quad (1b)$$

$$C_{IB} = \frac{r(1+r)^{N_y}}{D[(1+r)^{N_y} - 1]} \left( c_{ie} \sum_{j=1}^N ES_j^{rated} + c_{ip} \sum_{j=1}^N PE_j^{rated} + c_{con} \sum_{j=1}^N SP_j^{max} \right) \quad (1c)$$

$$C_{RB} = c_r \sum_{j=1}^N PE_j^{rated} + c_c \sum_{j=1}^N SP_j^{max} \quad (1d)$$

In (1),  $C_T$ ,  $C_{OP}$ ,  $C_{IB}$ , and  $C_{RB}$  are the total cost, network operation cost, storage investment cost, and storage repair cost, respectively. Parameters  $\Xi$ ,  $p^{\psi}$ ,  $N_g$ ,  $c_{em}$ ,  $cp_l$ ,  $N_l$ ,  $N$ ,  $cv_j$ ,  $c_{sp}$ ,  $c_{cap}$ ,  $\Delta t$ ,  $\eta_{LL}$ ,  $r$ ,  $N_y$ ,  $D$ ,  $c_{ie}$ ,  $c_{ip}$ ,  $c_{con}$ ,  $c_r$ , and  $c_c$  are the number of scenarios, scenario probability, number of generating units, emission cost, loss cost, number of lines, number of buses, voltage deviation penalty factor, renewable spillage cost, BESS energy cost per cycle, optimization time-step, leakage loss

factor of BESS, discount rate, BESS's lifetime, length of year (days), BESS energy investment cost, BESS power investment cost, BESS power conditioning system (PCS) investment cost, BESS's repair cost, and PCS repair cost, respectively. Variables  $Pl_{l,t}^{\psi}$ ,  $CG_{g,t}^{\psi}$ ,  $PG_{g,t}^{\psi}$ ,  $BV_{j,t}^{\psi}$ ,  $SP_{g,t}^{\psi}$ ,  $ES_j^{rated}$ ,  $Pd_{j,t}^{\psi}$ ,  $Pc_{j,t}^{\psi}$ ,  $ES_{j,t}^{\psi}$ ,  $PE_j^{rated}$ , and  $SP_j^{max}$  represent line loss, the linearized fuel cost function, active power output of the generator, bus voltage deviation, solar power spillage, BESS energy rating, BESS discharge power, BESS charge power, energy stored in BESS, power rating of BESS, and power rating of PCS, respectively. The constraints imposed on (1) are as follows:

$$\sum_{g=1}^{N_g} PG_{g,t}^{\psi} + \sum_{g=1}^{N_g} (PS_{g,t}^{\psi} - SP_{g,t}^{\psi}) + \sum_{j=1}^N (Pd_{j,t}^{\psi} - Pc_{j,t}^{\psi}) = \sum_{j=1}^N PD_{j,t}^{\psi} + \sum_{l=1}^{N_l} Pl_{l,t}^{\psi}, \forall t, \psi. \quad (2)$$

$$PG_{j,t}^{\psi} + PS_{j,t}^{\psi} - SP_{j,t}^{\psi} - PD_{j,t}^{\psi} + Pd_{j,t}^{\psi} - Pc_{j,t}^{\psi} = \sum_{k=1}^N \{ (1 + \Delta V_{j,t}^{\psi} + \Delta V_{k,t}^{\psi}) G_{j,k} + (\delta_{j,t}^{\psi} - \delta_{k,t}^{\psi}) B_{j,k} \}, \forall j, t, \psi. \quad (3)$$

$$QG_{j,t}^{\psi} + QS_{j,t}^{\psi} - QDL_{j,t}^{\psi} - st_{j,t}^{\psi} QDC_j + Qdis_{j,t}^{\psi} = \sum_{k=1}^N \{ (\delta_{j,t}^{\psi} - \delta_{k,t}^{\psi}) G_{j,k} - (1 + \Delta V_{j,t}^{\psi} + \Delta V_{k,t}^{\psi}) B_{j,k} \}, \forall j, t, \psi. \quad (4)$$

$$0 \leq SP_{g,t}^{\psi} \leq PS_{g,t}^{\psi}, \forall g, t, \psi. \quad (5)$$

$$(PS_{g,t}^{\psi})^2 + (QS_{g,t}^{\psi})^2 \leq (SS_g^{max})^2, \forall g, t, \psi. \quad (6)$$

$$-SS_g^{max} \leq QS_{g,t}^{\psi} \leq SS_g^{max}, \forall g, t, \psi. \quad (7)$$

$$\Delta V_{1,t}^{\psi} = 0, \delta_{1,t}^{\psi} = 0, \forall t, \psi. \quad (8)$$

$$\Delta V_j^{min} \leq \Delta V_{j,t}^{\psi} \leq \Delta V_j^{max}, \forall t, j \in \{2, \dots, N\}, \psi. \quad (9)$$

In (2)-(9),  $PS_{g,t}^{\psi}$ ,  $\Delta V_{j,t}^{\psi}$ ,  $G_{j,k}$ ,  $\delta_{j,t}^{\psi}$ ,  $B_{j,k}$ ,  $QG_{j,t}^{\psi}$ ,  $QS_{j,t}^{\psi}$ ,  $PD_{j,t}^{\psi}$ ,  $QDL_{j,t}^{\psi}$ ,  $QDC_j$ ,  $st_{j,t}^{\psi}$ , and  $Qdis_{j,t}^{\psi}$  represent the solar power output, bus voltage deviation, bus admittance matrix's real part, bus angle, bus admittance matrix's imaginary part, reactive power dispatch, reactive power output of solar resource, active power demand, inductive power demand, constant capacitive power demand, binary status variable, and BESS reactive power dispatch. Piecewise linearization of  $CG_{g,t}^{\psi}$ , and ramping and power dispatch constraints related to conventional generation have also been modeled in this research. The original non-linear power flow equations are appropriately linearized using the logic proposed in [23]. The original non-convex active power loss equations are piecewise linearized based on [24]. Additional constraints on BESS operation are:

$$\sum_{j=1}^N Pc_{j,t}^{\psi} \leq \sum_{j=1}^N SP_{j,t}^{\psi}, \forall j, t, \psi. \quad (10)$$

$$0 \leq \eta_{j,t}^c Pc_{j,t}^{\psi} \leq PE_j^{rated}, 0 \leq \frac{Pd_{j,t}^{\psi}}{\eta_{j,t}^d} \leq PE_j^{rated}, \forall j, t, \psi. \quad (11)$$

$$0 \leq PE_j^{rated} \leq d_j^{BESS} PE_j^{rated,max}, \forall j. \quad (12)$$

$$CDis_{j,1}^{\psi} = CDis_{j,0}^{\psi} + \frac{Pd_{j,1}^{\psi}}{\eta_{j,1}^d} \Delta t, \forall j, \psi. \quad (13)$$

$$CDis_{j,t}^{\psi} = CDis_{j,t-1}^{\psi} + \frac{Pd_{j,t}^{\psi}}{\eta_{j,t}^d} \Delta t, \forall j, t \geq 2, \psi. \quad (14)$$

$$CDis_{j,t}^{\psi} \leq PE_j^{rated} DT_j^{max}, \forall j, t, \psi. \quad (15)$$

$$SOC_{j,t}^\psi - (1 - \varpi)SOC_{j,t-\Delta t}^\psi - \eta_{j,t-\Delta t}^c Pc_{j,t-\Delta t}^\psi \Delta t + \frac{Pd_{j,t-\Delta t}^\psi}{\eta_{j,t-\Delta t}^d} \Delta t = 0, \forall j, t, \psi. \quad (16)$$

$$SOC_j^{min} \leq SOC_{j,t}^\psi \leq SOC_j^{max}, \forall j, t, \psi. \quad (17)$$

$$ES_{j,t}^\psi = SOC_{j,t}^\psi ES_j^{rated}, 0 \leq ES_{j,t}^\psi \leq ES_j^{rated}, \forall j, t, \psi. \quad (18)$$

$$0 \leq ES_j^{rated} \leq d_j^{BESS} ES_j^{rated,max}, \forall j \in \{1, \dots, N\}. \quad (19)$$

In (10)-(19), variables  $\eta_{j,t}^c$ ,  $\eta_{j,t}^d$ ,  $d_j^{BESS}$ ,  $CDis_{j,t}^\psi$ , and  $SOC_{j,t}^\psi$  represent the charging efficiency of BESS, discharging efficiency of BESS, binary siting decision variable, cumulative energy discharged by BESS at a time-instant, and SOC, respectively. Parameters  $DT_j^{max}$  and  $\varpi$  represent the maximum BESS discharge duration and self-discharge rate, respectively. It should be noted that the bi-linear term  $SOC_{j,t}^\psi ES_j^{rated}$  in (18) is linearized by using McCormick envelopes [25] while using the MILP solver. Apart from (10)-(19), charging/discharging powers of VRF BESS should be constrained to remain within its maximum absorption/delivering power [26]. Additional constraints on the BESS's reactive power control capability are found in [27].

### III. LINEAR PROGRAMMING (LP) OPTIMIZATION MODELS FOR LI AND VRF BESS

In this section, we build accurate LP operation models of the original non-linear LI and VRF BESS models for integration into the proposed scenario-based optimal BESS planning model from Section II. The non-linearity and non-convexity from the non-linear LI and VRF BESS models primarily gets introduced in constraints (11) and (16) through the terms  $\eta_{j,t}^c Pc_{j,t}^{s,\psi}$  and  $\frac{Pd_{j,t}^{s,\psi}}{\eta_{j,t}^d}$ , henceforth referred to as functions  $F1_t$  and  $F2_t$ , respectively, for VRF BESS, and  $F3_t$  and  $F4_t$ , respectively, for LI BESS (we omit superscripts  $s$ ,  $\psi$  and  $j$  for ease of representation). It should be noted that  $F1_t$ ,  $F2_t$ ,  $F3_t$  and  $F4_t$  are bivariate non-linear functions that vary as a function of SOC and charging/discharging power [13]; this non-linear dependence is clearly observed in Fig. 1.

We now develop the LP models only for  $F1_t$  and  $F2_t$  representing the charging and discharging operation of the VRF BESS, respectively. The convex LP models for  $F3_t$  and  $F4_t$  are formulated in a similar manner and are not shown here due to space constraints. One can use the mathematical expression for function  $F1_t(Pc_t, SOC_t)$  to generate a certain number of sampling points [13], [15]. These samples can then be used to create a linear convex approximation of  $F1_t$ . For every tuple  $[F1_t, Pc_t, SOC_t]^T$ ,  $N$  samples are generated; each sample is represented by  $[F1_t^n, \overline{Pc}_t^n, \overline{SOC}_t^n]^T$ . The number and range of the samples should be judiciously selected such that one is able to accurately capture the range of variation of  $F1_t$  (shown in Fig. 1(a)), while maintaining a balance between accuracy and computational burden. The linear convex model for  $F1_t$  is formulated in (20)-(22).

$$F1_t = \sum_n \overline{F1}_{n,t} a_{n,t}, Pc_t = \sum_n \overline{Pc}_{n,t} a_{n,t}, SOC_t = \sum_n \overline{SOC}_{n,t} a_{n,t}, \forall t. \quad (20)$$

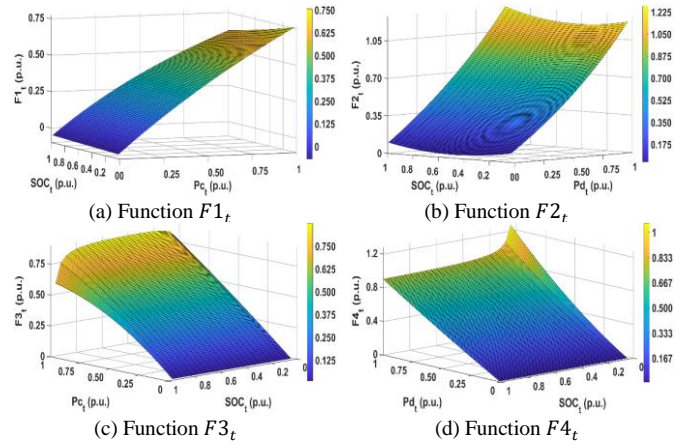


Fig. 1. Surface plots of bivariate non-linear functions  $F1_t$  to  $F4_t$ .

$$\sum_n a_{n,t} = 1, \forall t. \quad (21)$$

$$a_{n,t} \geq 0, \forall n \in N, t. \quad (22)$$

In a similar manner, the linear convex model for  $F2_t$  can be formulated in (23)-(25).

$$F2_t = \sum_u \overline{F2}_{u,t} b_{u,t}, Pc_t = \sum_u \overline{Pc}_{u,t} b_{u,t}, SOC_t = \sum_u \overline{SOC}_{u,t} b_{u,t}, \forall t. \quad (23)$$

$$\sum_u b_{u,t} = 1, \forall t. \quad (24)$$

$$b_{u,t} \geq 0, \forall u \in U, t. \quad (25)$$

where,  $a_{n,t}$  and  $b_{u,t}$  represent the  $n^{th}$  and  $u^{th}$  continuous variables related to each sample in sample sets  $N$  and  $U$ , respectively. Finally, in order to ensure that the BESSs do not charge and discharge simultaneously, each of the sample sets for  $F1_t$ ,  $F2_t$ ,  $F3_t$ , and  $F4_t$  must have two samples denoted by  $[0,1,0]^T$  and  $[0,0,0]^T$ , where the numbers  $\{0,1\}$  denote the corresponding values in p.u.

### IV. NUMERICAL RESULTS

We apply the developed BESS allocation scheme to a 2604-bus system representing the actual power transmission network of a U.S. state. This system has a total generation capacity of 24,840 MW and total active power demand of 24,773 MW. Current and future locations of solar farms in this system were provided by a power utility operating in the U.S. Southwest. The system's PV penetration level as a percentage of total system load was fixed at  $\sim 50\%$ . 100 representative scenarios of solar PV and load outputs were generated next. GUROBI is used to solve the scenario-based mixed-integer linear programs (MILPs) using a CPU with 3.6 GHz, Intel® Core™ i7-9700K 8-core processor and 64 GB RAM. Key parameter values used in this paper are found in Appendix B of [21]. For creating the LP BESS models described in Section III, 15, 13, 25, and 17 sampling points were used for approximating  $F1_t$ ,  $F2_t$ ,  $F3_t$ , and  $F4_t$ , respectively.

Four modeling approaches are considered in this study: *Model (a)*: non-linear programming models for both LI and VRF BESSs based on the non-linear equations for  $F1$ ,  $F2$ ,  $F3$ , and  $F4$  [13]; *Model (b)*: traditional constant-efficiency BESS

model (used in [3]-[12]) for LI and VRF BESSs; the charging and the discharging efficiencies for LI BESS and VRF BESSs are held constant at 92% and 82% [2], respectively; *Model (c)*: MILP models for both LI and VRF BESSs; the bivariate piecewise linearization approach described in [28] is used to build the MILP optimization formulations for  $F1$ ,  $F2$ ,  $F3$ , and  $F4$ ; and *Model (d)*: LP models for both LI and VRF BESSs that were developed in Section III. The BESS allocation results for the four BESS modeling approaches are shown in Table I.

TABLE I. OPTIMAL BESS ALLOCATION RESULTS CONSIDERING FOUR MODELING APPROACHES

Model	BESS allocation: Total MW (#buses)		Solution time (hours)
	LI	VRF	
(a)	3,857.92 (198)	2,383.62 (176)	111.446
(b)	2,008.02 (165)	1,122.63 (147)	2.331
(c)	2,751.60 (198)	1,538.40 (176)	58.477
(d)	2,752.19 (198)	1,539.11 (176)	4.149

We make the following observations from Table I:

- *Model (a)*: This modeling approach is the most realistic among the four approaches. However, in this model, one has to solve a non-convex mixed-integer non-linear program (MINLP), which results in locally optimal (or sub-optimal) solutions and long computation times. The MINLP version of the formulation given by (1)-(19) (without the LP BESS models from Section III) is solved for the 2,604-bus system by using KNITRO [29]. KNITRO can ensure optimality of solutions only when the constraints and objective function are convex, otherwise, it generates sub-optimal solutions using heuristic methods [29]. It is clear from Table I that the allocated BESS capacities and the CPU time for this model (approximately 111 hours) are the highest among the four modeling approaches.
- *Model (b)*: Since this model assumes constant efficiency for BESSs, it *appears* to give the best result among the four models, both in terms of BESS allocation as well as solution time. However, the results obtained using this model may not be very realistic since Fig. 1 clearly shows that the efficiencies of both BESS types vary non-linearly with charging/discharging power and SOC. This constant efficiency model captures the VRF and LI BESS operation when the efficiencies are very high but is unable to correctly capture them when the BESS charging/discharging efficiencies are relatively low. This optimistic assumption of constant high efficiencies for both BESSs results in the lowest BESS capacity being allocated at the candidate system buses. Since this model is the simplest among the four models in terms of number of constraints and variables, it results in the shortest solution time.
- *Model (c)*: This model is an improvement over Model (a) since the problem of non-linearity and non-convexity is resolved by the bivariate piece-wise linearization of  $F1$ ,  $F2$ ,  $F3$ , and  $F4$ , which results in near-globally optimal solutions. It is also an improvement over Model (b) as it does not assume a constant efficiency for the BESSs. As such, one can observe that the BESS allocation results for this model lie in between the sub-optimal solution generated by Model (a) and the optimistic solution generated by Model

(b). However, binary variables in large numbers get introduced in the BESS models by the *triangle method* [28] which results in the second-longest solution time.

- *Model (d)*: The BESS allocation results obtained using this convex model are slightly higher from those obtained in Model (c) since it does away with the binary variables associated with the building of LPs for  $F1$ ,  $F2$ ,  $F3$ , and  $F4$  as described in Section III. However, by doing so, the solution time is significantly reduced in comparison to Model (c). Therefore, one can conclude that Model (d) is able to provide an ideal balance of model accuracy, convexity, and computational performance for optimal BESS allocation in large transmission networks.

Table II compares the costs related to (1) with regards to the four BESS modeling techniques. A comparison is presented across Models (a) to (d) considering network operation metrics (average and maximum voltage deviations); annual network operation costs; and BESS investment and repair costs and payback periods. More specifically, we utilize the discounted payback period (DPP) [30] for comparison.

TABLE II. TECHNO-ECONOMIC COMPARISON OF FOUR BESS MODELING APPROACHES

	Model (a)	Model (b)	Model (c)	Model (d)
Network operation metrics (p.u.)				
Avg. voltage deviation	0.015	0.015	0.016	0.017
Max. voltage deviation	0.028	0.028	0.028	0.030
Network operation costs (M\$)				
Conventional generation	106.69	107.12	109.59	109.59
Emission	7.79	7.82	8.00	8.00
Renewable spillage	31.19	31.31	32.04	32.04
Active power loss	21.84	21.93	22.43	22.43
BESS operation	61.11	61.35	62.77	62.77
BESS investment and repair costs and DPP				
Investment (M\$)	688.67	484.24	537.52	538.05
Repair (M\$)	110.19	79.011	87.71	87.79
DPP (years)	12.01	8.42	9.32	9.33

The following observations are made from Table II:

- *Model (a)*: As observed previously, this model introduces non-convexity into the optimal BESS allocation problem, which generates sub-optimal solutions. Therefore, the solutions generated by this model cannot be considered trustworthy from the perspective of a transmission system planner. It should be noted that this model generates the highest investment and repair costs, and DPP.
- *Model (b)*: This model *appears* to generate optimal techno-economic benefits among the four models as its DPP is the lowest. However, this convex model is not very realistic as it assumes the charging/discharging efficiency to be uniformly high for both LI and VRF BESSs. This does not give an accurate representation of the BESS investment and repair costs required, and consequently, the network operational benefits which are gained from this investment may be overly optimistic.
- *Models (c) and (d)*: Model (c) is an improvement over Models (a) and (b) from the convexity and accuracy viewpoints, respectively. Therefore, solutions generated by this model can be considered trustworthy from the

transmission planner’s perspective. Even though Model (d) is an LP approximation of Model (c), one can observe that the results generated using Model (d) are very close to those of Model (c). The key reason for the aforementioned closeness in results lies in the fact that the number and range of samples are carefully selected (as described in Section III) to ensure the optimality of BESS planning results with acceptable solution times.

## V. CONCLUSIONS

In this paper, we developed LP optimization models for two diverse BESS technologies (VRF and LI) and integrated the models into a scenario-based optimal BESS allocation framework. Appropriate linearization of the overall BESS allocation framework was carried out for ensuring near-global optimality and scalability. The performance of the proposed BESS allocation approach was validated using a real U.S. transmission network. The performance of the LP optimization models was compared with three other BESS models; it was found that the LP optimization model provided an ideal balance from the model accuracy, convexity, and computational performance viewpoints. This research builds the foundation for a *comprehensive and computationally efficient framework for co-optimizing the allocation of VRF and LI BESSs in practical transmission & distribution (T&D) networks* (which are massive in size and complexity), while accounting for uncertainties due to system load and presence of renewable generation.

## REFERENCES

- [1] US Solar Market Insight (SEIA) [Online]. Available: <https://www.seia.org/us-solar-market-insight>.
- [2] Electricity Storage and Renewables: Costs and Markets to 2030 (IRENA) [Online]. Available: [http://www.irena.org/media/Files/IRENA/Agency/Publication/2017/Oct/IRENA\\_Electricity\\_Storage\\_Costs\\_2017.pdf](http://www.irena.org/media/Files/IRENA/Agency/Publication/2017/Oct/IRENA_Electricity_Storage_Costs_2017.pdf).
- [3] R. F. Blanco, Y. Dvorkin, B. Xu, Y. Wang, and D. S. Kirschen, “Optimal energy storage siting and sizing: a WECC case study,” *IEEE Trans. Power Syst.*, vol. 8, no. 2, pp. 733–743, Apr. 2017.
- [4] S. Wogrin and D. F. Gayme, “Optimizing storage siting, sizing, and technology portfolios in transmission-constrained networks,” *IEEE Trans. Power Syst.*, vol. 30, no. 6, pp. 3304–3313, Nov. 2015.
- [5] D. Yacar, D. A. T. Arango, and S. Wogrin, “Storage allocation and investment optimization in transmission-constrained networks considering losses and high renewable penetration,” *IET Renew. Power Gener.*, vol. 12, no. 16, pp. 1949–1956, Dec. 2018.
- [6] T. Qiu, B. Xu, Y. Wang, Y. Dvorkin, and D. S. Kirschen, “Stochastic multistage coplanning of transmission expansion and energy storage,” *IEEE Trans. Power Syst.*, vol. 32, no. 1, pp. 643–651, Jan. 2017.
- [7] B. Xu, *et al.*, “Scalable planning for energy storage in energy and reserve markets,” *IEEE Trans. Power Syst.*, vol. 32, no. 6, pp. 4515–4527, Nov. 2017.
- [8] Y. Dvorkin, *et al.*, “Co-planning of investments in transmission and merchant energy storage,” *IEEE Trans. Power Syst.*, vol. 33, no. 1, pp. 245–256, Jan. 2018.
- [9] S. M. M. Bonab, I. Kamwa, A. Moeini, and A. Rabiee, “Voltage security-constrained stochastic programming model for day-ahead BESS schedule in co-optimization of T&D systems,” *IEEE Trans. Sustain. Energy (Early Access)*, pp. 1–12, Jan. 2019.
- [10] Y. Zhang, Y. Xu, H. Yang, and Z. Y. Dong, “Voltage regulation-oriented co-planning of distributed generation and battery storage in active distribution networks,” *Int. J. Electr. Power Energy Syst.*, vol. 105, pp. 79–88, Feb. 2019.
- [11] A. Jalali and M. Aldeen, “Risk-based stochastic allocation of ESS to ensure voltage stability margin for distribution systems,” *IEEE Trans. Power Syst.*, vol. 34, no. 2, pp. 1264–1277, Mar. 2019.
- [12] H. A. Hejazi and H. M. Rad, “Energy storage planning in active distribution grids: a chance-constrained optimization with non-parametric probability functions,” *IEEE Trans. Smart Grid*, vol. 9, no. 3, pp. 1972–1985, May 2018.
- [13] T. A. Nguyen, D. A. Copp, R. H. Byrne, and B. Chalamala, “Market-evaluation of energy storage systems incorporating technology-specific nonlinear models,” *IEEE Trans. Power Syst.*, vol. 34, no. 5, pp. 3706–3715, Sep. 2019.
- [14] A. Sakti, *et al.*, “Enhanced representations of Lithium-ion batteries in power systems models and their effect on the valuation of energy arbitrage applications,” *J. Power Sources*, vol. 342, pp. 279–291, Feb. 2017.
- [15] A. J. G. Castellanos, D. Pozo, and A. Bischi, “Non-ideal linear operation model for Li-ion batteries,” *IEEE Trans. Power Syst. (Early Access)*, pp. 1–11, Jul. 2019.
- [16] H. Pandžić and V. Bobanac, “An accurate charging model of battery energy storage,” *IEEE Trans. Power Syst.*, vol. 34, no. 2, pp. 1416–1426, Mar. 2019.
- [17] D. Rosewater, S. Ferreira, D. Schoenwald, J. Hawkins, and S. Santoso, “Battery energy storage state-of-charge forecasting: Models, optimization, and accuracy,” *IEEE Trans. Smart Grid*, vol. 10, no. 3, pp. 2453–2462, May 2019.
- [18] J. M. Cabello, X. Roboam, S. Junco, E. Bru, and F. Lacressonniere, “Scaling electrochemical battery models for time-accelerated and size-scaled experiments on test-benches,” *IEEE Trans. Power Syst.*, vol. 32, no. 6, pp. 4233–4240, Nov. 2017.
- [19] A. A. Mamun, Z. Liu, D. M. Rizzo, and S. Onori, “An integrated design and control optimization framework for hybrid military vehicle using Lithium-ion battery and supercapacitor as energy storage devices,” *IEEE Trans. Transport. Electrific.*, vol. 5, no. 1, pp. 239–251, Mar. 2019.
- [20] A. Pinceti, O. Kosut, and L. Sankar, “Data-driven generation of synthetic load datasets preserving spatio-temporal features,” in *IEEE Power Energy Soc. Gen. Meet.* (Accepted), Atlanta, GA, USA, Aug. 4–8, 2019, pp. 1–5.
- [21] M. Padhee, A. Pal, C. Mishra, and K. A. Vance, “A fixed-flexible BESS allocation scheme for transmission networks considering uncertainties,” *IEEE Trans. Sustain. Energy* (accepted), pp. 1–13, Sep. 2019. [Online]. Available: <https://arxiv.org/abs/1905.07536>.
- [22] Y. Wang, Y. Liu, and D. S. Kirschen, “Scenario reduction with submodular optimization,” *IEEE Trans. Power Syst.*, vol. 32, no. 3, pp. 2479–2480, May 2017.
- [23] J. Wang, N. Zhang, C. Kang, and Q. Xia, “A state-independent linear power flow model with accurate estimation of voltage magnitude,” *IEEE Trans. Power Syst.*, vol. 32, no. 5, pp. 3607–3617, Sep. 2017.
- [24] H. Zhang, G. T. Heydt, V. Vittal, and J. Quintero, “An improved network model for transmission expansion planning considering reactive power and network losses,” *IEEE Trans. Power Syst.*, vol. 28, no. 3, pp. 3471–3479, Aug. 2013.
- [25] Envelope approximations for global optimization (YALMIP) [Online]. Available: <https://yalmip.github.io/tutorial/envelopesinbmibnb/>.
- [26] J. Lei and Q. Gong, “Operating strategy and optimal allocation of large-scale VRB energy storage system in active distribution networks for solar/wind power applications,” *IET Gener. Transm. Distrib.*, vol. 11, no. 9, pp. 2403–2411, Jul. 2017.
- [27] A. Gabash and P. Li, “Active-reactive optimal power flow in distribution networks with embedded generation and battery storage,” *IEEE Trans. Power Syst.*, vol. 27, no. 4, pp. 2026–2035, Nov. 2012.
- [28] C. D’Ambrosio, A. Lodi, and S. Martello, “Piecewise linear approximation of functions of two variables in MILP models,” *Oper. Res. Lett.*, vol. 38, no. 1, pp. 39–46, Jan. 2010.
- [29] Mixed-integer nonlinear programming (Artelys) [Online]. Available: [https://www.artelys.com/docs/knitro/2\\_userGuide/minlp.html](https://www.artelys.com/docs/knitro/2_userGuide/minlp.html).
- [30] S. Yard, “Developments of the payback period,” *Int. J. Prod. Econ.*, vol. 67, no. 2, pp. 155–167, Sep. 2000.